ECOLOGY

Precipitation and temperature drive continental-scale patterns in stream invertebrate production

C. J. Patrick¹*, D. J. McGarvey², J. H. Larson³, W. F. Cross⁴, D. C. Allen⁵, A. C. Benke⁶, T. Brey⁷, A. D. Huryn⁶, J. Jones⁸, C. A. Murphy⁹, C. Ruffing¹⁰, P. Saffarinia¹¹, M. R. Whiles¹², J. B. Wallace¹³, G. Woodward¹⁴

Secondary production, the growth of new heterotrophic biomass, is a key process in aquatic and terrestrial ecosystems that has been carefully measured in many flowing water ecosystems. We combine structural equation modeling with the first worldwide dataset on annual secondary production of stream invertebrate communities to reveal core pathways linking air temperature and precipitation to secondary production. In the United States, where the most extensive set of secondary production estimates and covariate data were available, we show that precipitation-mediated, low-stream flow events have a strong negative effect on secondary production. At larger scales (United States, Europe, Central America, and Pacific), we demonstrate the significance of a positive two-step pathway from air to water temperature to increasing secondary production. Our results provide insights into the potential effects of climate change on secondary production and demonstrate a modeling framework that can be applied across ecosystems.

Copyright © 2019
The Authors, some rights reserved; exclusive licensee
American Association for the Advancement of Science. No claim to original U.S. Government Works. Distributed under a Creative
Commons Attribution
NonCommercial
License 4.0 (CC BY-NC).

INTRODUCTION

Secondary production is the generation of new heterotrophic biomass over time. It is a fundamental ecosystem process because it requires the consumption of basal energetic sources while sustaining consumers at higher trophic levels in both aquatic and terrestrial food webs (1-5). Secondary production can be used to assess higher-level responses to environmental change (6) and human perturbations (7, 8), including ecosystem services such as water filtration (9, 10) and fisheries production (11, 12). Understanding how secondary production may respond to climate change is therefore essential. Invertebrates are diverse and productive members of most food webs and comprise the majority of metazoan diversity globally. Previous research has characterized local-scale effects of temperature on individual invertebrate taxa (13-15), but the potential effects of continental- to global-scale shifts in temperature and precipitation on entire communities of invertebrate secondary producers are largely unknown (16).

Identifying drivers of annual community secondary production (ACSP), defined as the sum of annual production of all invertebrate populations within a community (17), is particularly challenging because individual- and species-level processes do not always scale up to the community level in a direct additive manner. Functional

¹Department of Life Sciences, Texas A&M University, 6300 Ocean Drive, Corpus Christi, TX 78412, USA. ²Center for Environmental Studies, Virginia Commonwealth University, Richmond, VA 23284, USA. ³Upper Midwest Environmental Sciences Center, U.S. Geological Survey, 2630 Fanta Reed Rd., La Crosse, WI 54603, USA. ⁴Department of Ecology, Montana State University, Bozeman, MT 59717, USA. ⁵Department of Biology, University of Oklahoma, 730 Van Vleet Oval, Norman, OK 73019, USA. ⁶University of Alabama, Tuscaloosa, AL 35487, USA. ⁷Alfred Wegener Institute, Helmholtz Center for Polar and Marine Research, Bremerhaven & Helmholtz Institute for Functional Marine Biodiversity at the University of Oldenburg, Oldenburg, Germany. ⁸University of Alaska Fairbanks, Fairbanks, AK 99775, USA. ⁹Department of Fisheries and Wildlife, Oregon State University, Corvallis, OR 97331, USA. ¹⁰University of British Columbia, 2329 West Mall, Vancouver, BC V6T 1Z4, Canada. ¹¹University of California, Riverside, 900 University Ave., Riverside, CA 92521, USA. ¹²Department of Zoology, Cooperative Wildlife Research Laboratory and Center for Ecology, Southern Illinois University, Carbondale, IL 62901, USA. ¹³Department of Entomology and Odum School of Ecology, University of Georgia, Athens, GA 30602, USA. ¹⁴Department of Life Sciences, Imperial College London, Silwood Park Campus, Buckhurst Rd., Ascot, Berkshire SL5 7PY, UK.

*Corresponding author. Email: christopher.patrick@tamucc.edu

redundancy in the roles that species play within a food web can offset environmental perturbations via compensatory effects on overall production (18). For this reason, ACSP may be a more useful holistic indicator of the ecosystem-level effects of climate change than production rates of discrete taxa or functional groups. Unfortunately, studies of the effects of macroscale shifts in temperature and precipitation on ACSP, which are difficult to conduct in experimental settings, are rare [but see (19)].

Previous research in stream and river ecosystems provides a unique opportunity to further understand the linkages between ACSP and climate. When compared to other types of ecosystems, empirical studies of ACSP in streams and rivers are relatively common (20, 21). We leveraged this previous work by combining a literature review on freshwater ACSP with geospatial analysis, hydrologic modeling, and structural equation modeling (SEM) to test hypotheses linking air temperature and precipitation to ACSP in lotic ecosystems. Our ultimate goal was to build a systems-level framework that can be expanded or refined in future research and used to predict climate-driven changes in ACSP.

Our study focuses primarily on the effects of air temperature and precipitation on ACSP because both factors are closely linked to physicochemical conditions in freshwater ecosystems. Air temperature is a principal driver of water temperature in lotic systems (22), and water temperature stimulates in-stream primary production (23, 24); this two-step pathway may link air temperature to ACSP (25). Precipitation effects on ACSP may be mediated by hydrology, which is a key determinant of habitat stability for benthic invertebrates that reside on or within streambed substrates. Stable flows promote well-sorted substrates that support high invertebrate densities and allow extended growth periods (26, 27). In contrast, systems that experience extreme floods and/or droughts tend to have low secondary production (7, 28, 29).

We began this study with an extensive literature review of empirical measurements of ACSP in lotic ecosystems and associated in situ covariates, such as water temperature and channel substrate characteristics. We then used a geographic information system to append spatially derived covariates, including land use, elevation,

slope, and local climate, to the ACSP data. Many environmental covariates were available for study sites within the United States, but only climate and elevation data were consistently available for sites outside of the United States. New hydrologic variables, such as minimum 30-day stream flow (the minimum average discharge that persists for 30 consecutive days), were then calculated by using existing covariates as predictors in statistical models (see Materials and Methods) and appended to the covariate data for U.S. sites. By combining covariates from multiple sources, we were able to expand the number of variables and causal pathways that we tested in models of ACSP

Links between climate and ACSP were then tested with a combination of traditional univariate regression analysis and SEM. The latter approach was central to our study because SEMs can be used to evaluate cause-and-effect relationships among discrete variables (30), can explicitly account for covariation among variables, and can simultaneously test systems-level hypotheses that are expressed as complex networks of interrelationships among variables (31). Development of SEMs of ACSP constitutes a significant advance, relative to previous reviews of aquatic secondary production (1, 32), because it allows us to evaluate multiple drivers of ACSP within a single integrative framework. In addition, this study demonstrates a novel yet general approach to integrate meta-analysis of published results, covariate data that were mined from independent sources and appended to published data, and statistical modeling (univariate regression and SEM) for the purpose of deriving greater insight from published information and creating new conceptual understanding of connections among suites of environmental and biotic variables.

Before model building and testing, we outlined an a priori hypothesis or "metamodel" (30) of systems-level links between major climate variables and ACSP (Fig. 1). Habitat stability and water temperature were predicted to be proximal drivers of ACSP. Hydrology (28), channel substrate (33), and land cover (34) were predicted to drive habitat stability. Air temperature (22), canopy shading (35), and stream channel size (36) were predicted to influence water temperature. Precipitation, latitude, and elevation were predicted to act as distal effects on ACSP, mediated through their effects on temperature and riparian vegetation.

Models were tested at two distinct spatial scales. First, we modeled ACSP at the continental scale, using only U.S. study sites. This allowed us to test complex cause-and-effect relationships using the full suite of environmental covariates that was assembled for U.S. sites. Second, we developed simpler ACSP models at a larger scale that included sites from Europe, Central and South America, and New Zealand. These inclusive models were constrained by the smaller number of environmental covariates that were available at all study sites, but they did allow us to test the generality of some key results from the U.S. models.

RESULTS AND DISCUSSION

Among all U.S. samples, ACSP spanned four orders of magnitude [35 to 612,231 mg ash-free dry mass (AFDM) m⁻² year⁻¹] and was strongly positively skewed [median, 9991; coefficient of variation (CV), 0.41; see Fig. 2A, inset]. A nearly identical distribution of ACSP was observed at the global scale (median, 9982; CV, 0.42; see Fig. 2B, inset). In U.S. streams, univariate regression analyses detected significant positive effects of mean annual water temperature, basin area, minimum 30-day flow, and percent urban development on

ACSP (Table 1), consistent with hypothesized links A, B, E, F, and H in Fig. 1. A significant negative effect was also detected for percent forest cover, as predicted by link C in the metamodel. Of the univariate relationships, water temperature had the strongest overall effect on ACSP (standardized effect size $\beta = 0.39$).

Nine covariates and 14 path links were retained in the final SEM for U.S. streams (Fig. 2A and Table 2). Of these, some paths were simple and predictable, such as the strong effect of air temperature on water temperature (37), the effects of latitude and elevation on air temperature, and the effect of precipitation on minimum 30-day discharge. However, other paths were more complex. For instance, the total effect of precipitation on water temperature included two paths: a direct positive link from precipitation to water temperature and a negative indirect link that was mediated by forest cover (precipitation \rightarrow forest cover \rightarrow water temperature; see Fig. 2A). This indirect effect of precipitation on water temperature may be attributed to wetter regions having comparatively dense forests with larger canopies and more extensive shading (38, 39) or enhanced evaporation (40).

The U.S. SEM confirmed many of the hypothesized pathways in the metamodel (Fig. 1), most notably the direct influence of base flow stability and water temperature on ACSP. Significant indirect effects of climate (air temperature and precipitation), the physical landscape (catchment elevation and basin area), and land cover (impervious surface area and forest cover) on ACSP were mediated through their direct effects on water temperature and base flow stability. The final inclusive SEM complimented the U.S. model by confirming that air temperature and precipitation have consistent, predictable effects on ACSP that are mediated by their direct effects on water temperature (Fig. 2B).

The positive effect of water temperature on ACSP in the U.S. and global models is perhaps intuitive, but our quantitative results raise pressing theoretical questions and can help to reconcile conflicting results from previous site-specific studies. The metabolic theory of ecology (MTE) predicts that standing stock biomass should decrease with increasing temperature, while the production-to-biomass (P:B) relationship should increase with temperature, resulting in no net change in secondary production (41). Some empirical support for this prediction is provided by observational meta-analyses (32) and controlled in situ stream warming experiments (16), but other studies have documented net positive effects of temperature on body size, growth rates, and total production (1, 25). Our results, which constitute the most comprehensive meta-analysis to date, indicate that the relationship between temperature and ACSP is net positive. Given that the MTE assumes constant resource supply, we posit that the mechanism responsible for the observed positive relationship between water temperature and ACSP may be a temperature-mediated increase in basal resources (42). Thus, we suggest that closer examination of the effect of basal resources on ACSP should be a priority area in future research (43-45).

Basal resources are likely to improve systems-level models of ACSP because food quality and quantity are already known to be fundamental determinants of individual growth (46-48) and of ACSP (49) in aquatic ecosystems. For instance, allochthonous leaf litter has low nutritional value, relative to autochthonous material, but can account for >90% of the annual variation in secondary production within temperate streams because it is so abundant (45, 50, 51). Allochthonous material was not included in our models because it was not measured at most study sites (see data file 2). However,

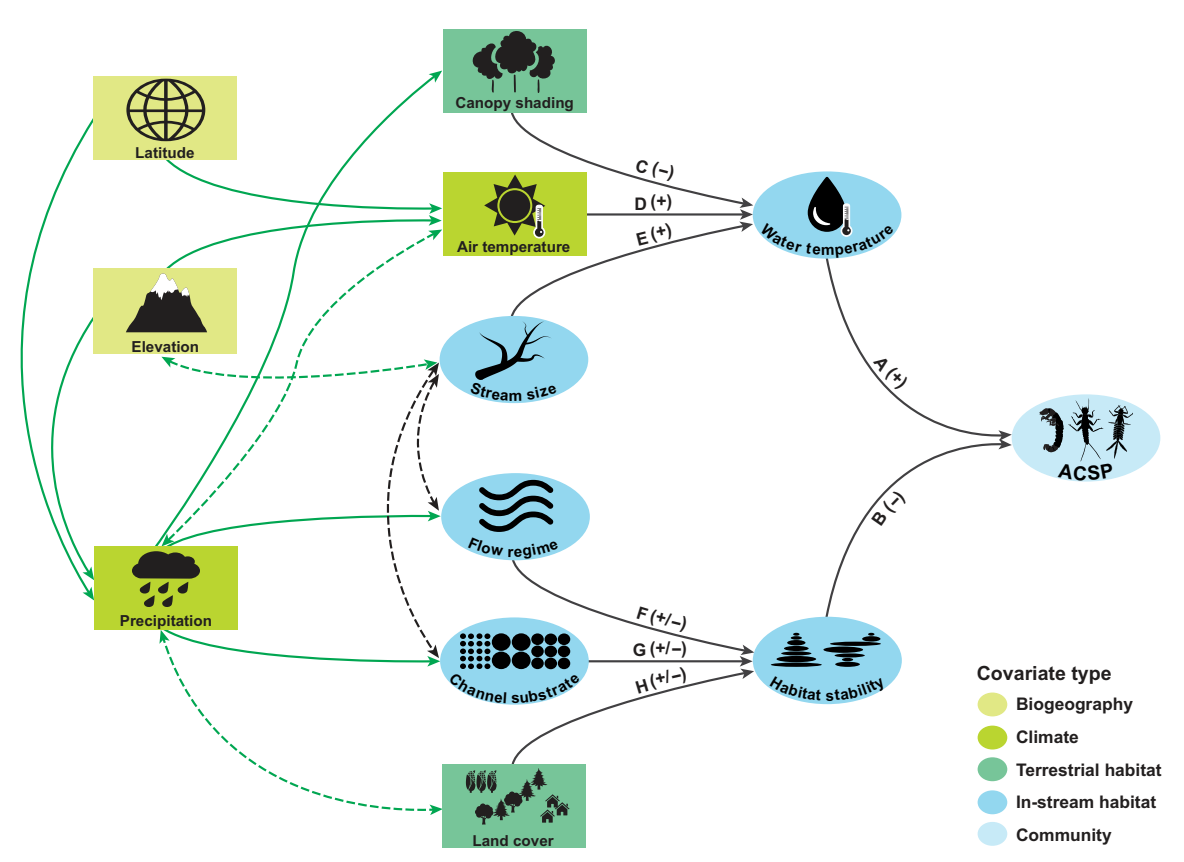


Fig. 1. Conceptual diagram or metamodel of major hypothesized influences on ACSP. Covariates that are external to stream ecosystems (i.e., exogenous variables) are indicated by rectangles. Covariates that are direct measures of in-stream conditions or processes (i.e., endogenous variables) are indicated by ovals. Each covariate is also recognized as one of five color-coded types (see inset key): biogeography, climate, terrestrial habitat, in-stream habitat, and community. Solid black arrows depict known causal effects among covariates. Arrow labels correspond to exemplar references [A (23, 25), B (26, 27), C (35, 94), D (22, 95), E (36, 96), F (7, 28), G (29, 33), H (34, 97)]. Parenthetic signs next to black arrow labels indicate that the relationship is expected to be positive (+), negative (-), or variable (+/-). Solid green arrows depict fundamental relationships that are expected but not explicitly documented here (e.g., the negative relationship between latitude and air temperature). Dashed arrows depict hypothesized covariation among variables.

using a subset of U.S. studies that measured both allochthonous organic material and ACSP (n=41), we detected a strong positive univariate relationship between coarse particulate organic matter (CPOM) and ACSP ($r^2=0.279, P<0.001$). Notably, CPOM accounted for more of the variation in ACSP than water temperature and habitat stability combined (in the U.S. SEM; see Fig. 2A). We are therefore confident that additional information on basal resources and the mechanisms that link them to climate (52-55) will enhance our ability to predict ACSP in changing climates.

Hydrology also stood out as a key regulator of ACSP. Results from U.S. streams indicated that discharge magnitude during dry or low flow periods (i.e., minimum 30-day flow) has a significant positive effect (β = 0.24) on ACSP (Fig. 2A and Table 1). While this is consistent with previous site-specific findings that environmental stability increases in-stream production (56–58), our study is the first to demonstrate this relationship at the continental scale. Hydrologic stability, as one dimension of environmental stability in lotic ecosystems, is known to have a significant effect on secondary production (59–62), particularly in drought-prone systems (63). However, the effect of hydrology did not extend to measures of flooding or "flashiness." These factors are important to invertebrates in some lotic ecosystems (26, 58, 64), but they did not have a significant effect on ACSP in our analyses. This may be due to variation

among communities in the response to flashiness, where naturally flashy streams are inhabited by organisms with adaptive traits that convey resilience (59, 65).

One notable difference between the U.S. and inclusive models was a significant positive effect of absolute latitude on ACSP; this link between latitude and ACSP, which was independent of a latitudinal effect on temperature, was detected in the inclusive model but not in the final U.S. model. The difference may be an artifact of the truncated range of latitudes among U.S. streams relative to the global range. However, it may also indicate that additional information on benthic community structure is needed to understand ACSP at global scales. Links between benthic diversity, biomass (66, 67), and secondary production (68, 69) have been documented in freshwater ecosystems, and benthic invertebrate diversity is known to vary with latitude (70, 71). Incorporating new dimensions of community structure, such as diversity and standing stock biomass, may therefore help to explain the effect of latitude on ACSP.

Moving forward, an obvious goal should be to increase the explained variation in ACSP. Coefficients of determination for ACSP were <0.25 in both the U.S. and global SEMs (Fig. 2)—a strong indication that some key variables were not included in the models. Here, our goal was to advance conceptual understanding of the systems-level drivers of ACSP by identifying causal pathways that link climate

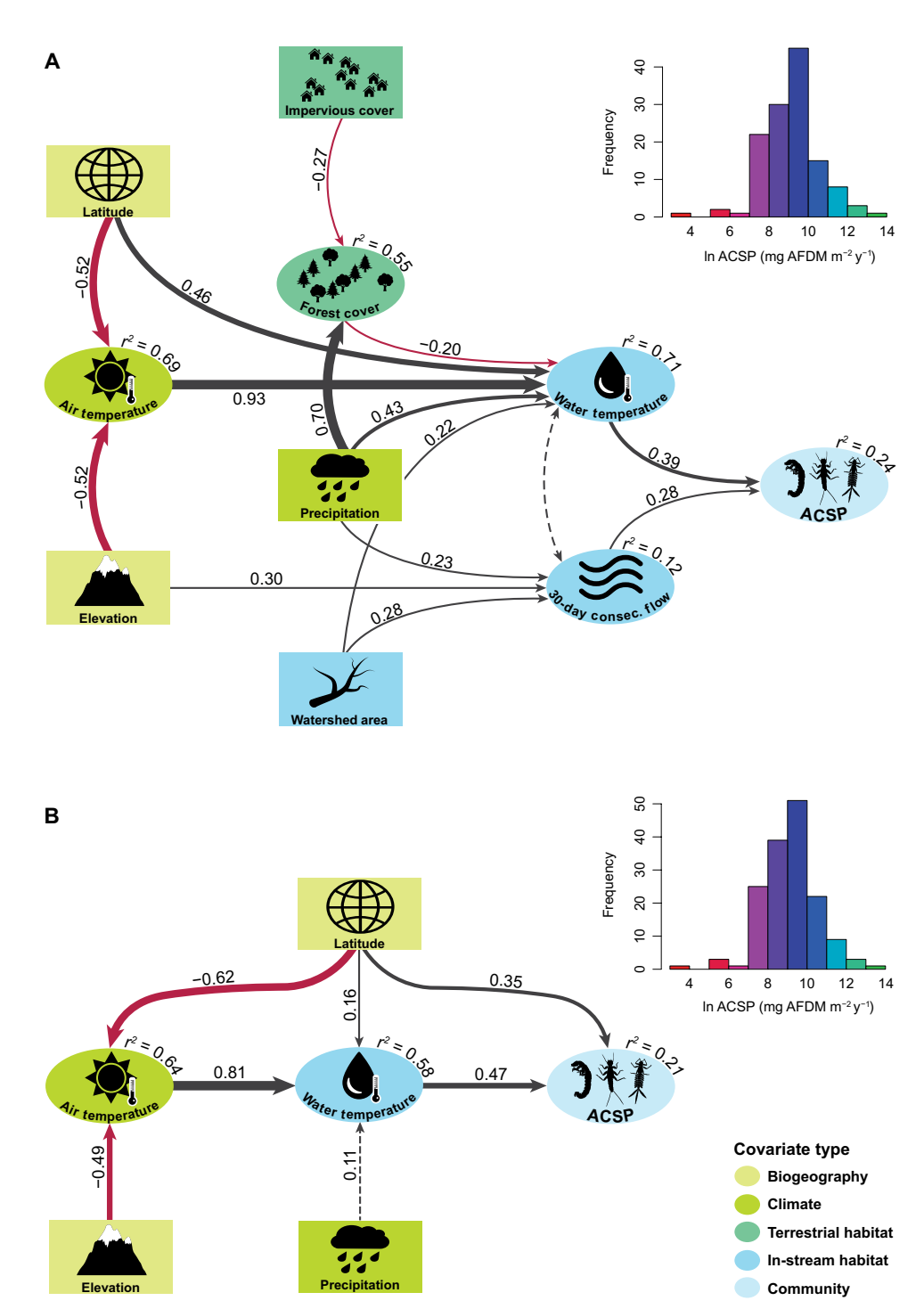


Fig. 2. SEMs of ACSP in streams and rivers. Models include an SEM for the U.S. (**A**) and for global streams and rivers (**B**). Exogenous variables are indicated by rectangles, and endogenous variables are represented by ovals. Coefficients of determination (r^2) are shown for all endogenous variables, and standardized path coefficients are shown for all modeled relationships. Positive and negative effects among variables are depicted by black and red arrows, respectively, with arrow widths proportional to effect sizes (i.e., path coefficients). In the U.S. model, significant covariance between mean annual water temperature ("Water temperature") and the minimum average discharge that persists for 30 consecutive days ("30-day consec. flow") is depicted by a dashed double-headed arrow. In the global model, the dashed arrow between mean annual precipitation ("Precipitation") and mean annual water temperature indicates a nominally significant (P = 0.09) effect; all other relationships in the U.S. and global models are significant at P = 0.05. Both the U.S. and global models satisfied each of the three model fit criteria, with significant $\chi^2 P$ values (U.S. = 0.06; global = 0.03), standardized root mean squared residuals (U.S. = 0.06; global = 0.02), and comparative fit index values (U.S. = 0.97; global > 0.99). Inset histograms show the distribution of natural log (In)–transformed ACSP at U.S. and global scales. Covariate types are as shown in Fig. 1.

Table 1. Comparison of effect sizes in univariate regression models of ACSP in U.S. streams. Unstandardized regression slopes (*b*) and standardized slopes (β) are each reported with 95% confidence intervals (shown in parentheses) as well as sample sizes (*n*) and coefficients of determination (r^2). Covariates shown in bold text have slopes (95% confidence intervals) that exclude zero and are therefore considered statistically significant.

Hypothesized effect	Covariate	n	b	β	r ²
Temperature	Mean annual air temperature	128	1.32 (-0.11 to 2.75)	0.16 (-0.01 to 0.34)	0.02
	Mean annual water temperature	107	1.32 (0.74 to 1.90)	0.39 (0.22 to 0.57)	0.15
Canopy shading	% Forest cover in catchment	128	−0.56 (−1.06 to −0.06)	−0.19 (−0.37 to −0.02)	0.03
Stream size	Basin area	128	0.10 (0.02 to 0.19)	0.21 (0.03 to 0.38)	0.03
	Mean annual discharge	102	0.04 (-0.03 to 0.11)	0.10 (-0.08 to 0.27)	<0.01
Hydrology	Flashiness	124	-0.23 (-0.64 to 0.19)	-0.10 (-0.27 to 0.08)	<0.01
•	CV discharge	124	-0.20 (-0.86 to 0.45)	-0.06 (-0.24 to 0.13)	0.01
	Minimum 30-day consecutive flow	124	1.36 (0.39 to 2.33)	0.24 (0.07 to 0.42)	0.05
Channel substrate	Average sediment size (unweighted)	88	-0.10 (-0.22 to 0.02)	-0.17 (-0.38 to 0.04)	0.02
	Average sediment size (weighted)	88	-0.12 (-0.24 to 0.00)	-0.20 (-0.41 to 0.01)	0.03
Land cover	Impervious surface in basin	124	3.24 (-0.19 to 6.67)	0.16 (-0.01 to 0.34)	0.02
	% Medium density urbanization in catchment	128	3.39 (1.11 to 5.68)	0.25 (0.08 to 0.42)	0.06
	% Crop cover in catchment	128	0.86 (-0.46 to 2.18)	0.11 (-0.06 to 0.29)	0.01

to ACSP; we did not seek to maximize explained variation in ACSP per se. The SEM allowed us to test the hypothesized linkages among variables (Fig. 1) in a critical and explicit way. Nevertheless, future progress will benefit from the addition and testing of new covariates and links between climate and ACSP.

Basal resource availability was previously noted as a priority research topic. Another focus area should be the role of anthropogenic stressors on ACSP. Previous research has reported a positive relationship between some land-use activities and ACSP that covaries with watershed area (72). Consistent with this earlier finding, we detected a positive relationship between watershed area and ACSP. However, when impervious surface area and agricultural land use were added to preliminary SEMs, we were unable to detect a significant influence of either variable on ACSP. The apparent lack of a strong land-use effect on ACSP may be a sampling artifact, as many of the study sites were located at field stations where human impacts were likely minimal. For example, 64% of all streams in the U.S. database were entirely unaffected by row-crop agriculture and only 7% of the U.S. streams flowed through watersheds, where rowcrop agriculture accounted for >10% of internal land use. Thus, the current ACSP database may be ill suited to evaluate land-use effects, leaving a key information gap to be filled.

Despite the limitations of the ACSP models, our results have clear implications for ecosystem function in the face of climate change. Climate models predict that over the next century, average air temperatures will continue to rise (73) and precipitation patterns will shift markedly (74, 75). Our models suggest that these changes will

have cascading effects on ACSP mediated through water temperature and discharge during dry periods. For instance, the SEMs predict that warming temperatures will tend to increase ACSP. However, the frequency and severity of low flow events are expected to increase in many ecosystems as subhumid regions transition to semiarid climates (75–77). If these systems are populated by invertebrates that lack physiological or life history traits that allow them to persist under drought conditions, temperature-driven increases in ACSP are likely to be offset by increased mortality or diminished recruitment.

In conclusion, we suggest that four key areas of research should now be pursued to advance understanding of ACSP. First, new ACSP data from undersampled regions are needed to determine whether the results presented here are applicable in other parts of the globe. Second, a better understanding of the roles that basal resources or other bottom-up trophic constraints play in regulating ACSP and how these basal factors are affected by climate is needed. Third, the effects of anthropogenic stressors should be incorporated in systemslevel models. Fourth, the general ACSP results should be tested using habitat-specific production estimates (3, 60, 62), paying special attention to account for differential effects on specific invertebrate traits or functional groups (78, 79). Addressing each of these needs will be a challenging and labor-intensive process, but we have shown that an enhanced understanding of the complex mechanisms that drive ACSP at continental to global scales is achievable when the efforts and data of many ecologists are integrated within an appropriate modeling framework.

Table 2. Direct and total effects of each driver on ACSP in the U.S. and global models. Total effects are calculated as the sum of the direct and indirect effects of the predictor on the response variable.

SEM model	Predictor	Response	Direct	Total effect
U.S. model	Water temperature	ACSP	0.39	0.39
	30-day consecutive flow	ACSP	0.28	0.28
	Precipitation	ACSP		0.18
	Air temperature	ACSP		0.36
	Impervious cover	ACSP		0.02
	Watershed area	ACSP		0.16
	Mean elevation	ACSP		-0.10
	Absolute latitude	ACSP		-0.01
•	Forest cover	ACSP		-0.08
Global model	Absolute latitude	ACSP	0.35	0.19
	Air temperature	ACSP		0.38
•	Mean elevation	ACSP		-0.19
•••••	Precipitation	ACSP		0.05
•	Water temperature	ACSP	0.47	0.47

MATERIALS AND METHODS

We used the following workflow: (i) perform a literature review of invertebrate ACSP studies; (ii) append environmental covariates to the ACSP data assembled in the literature review; (iii) use univariate regression to test significant relationships between key covariates and ACSP; and (iv) use SEM to identify causal pathways within networks of interacting covariates, thereby distinguishing direct from indirect drivers of ACSP (31). SEM analyses were conducted at two scales: streams throughout the United States and a global analysis of streams distributed across six continents (fig. S1). By first analyzing U.S. streams, we were able to use a large standardized set of environmental covariates in critical testing of the metamodel (Fig. 1). The global-scale analysis was limited by a reduced number of covariates, but it allowed us to examine the generality of some key pathways in the U.S. model.

Literature review

Potential sources of ACSP data were first identified through an ISI Web of Science search (keywords "stream OR streams OR creek OR lotic AND benthic OR benthos OR invertebrate OR macroinvertebrate AND production") that returned 468 sources (peerreviewed publications, government reports, or indexed theses). Each of these publications was then checked for compliance with three a priori criteria: (i) Data were exclusive to within-channel ACSP and did not include estimates of floodplain production; (ii) samples were inclusive of all locally occurring taxa and did not focus on a discrete subset of taxa or functional feeding groups; and (iii) ACSP estimates were inferred from repeat samples collected throughout the year [e.g., size frequency or cohort methods (17)], rather than P:B relationships (80). However, ACSP estimates inferred from P:B relationships were acceptable when used solely to "fill in" production estimates for rare or low biomass taxa that could not be partitioned into distinct size classes or cohorts. This screening process reduced the initial list of 468 publications to 56, most of which included ACSP estimates for multiple sites; from

the final 56 publications, we obtained 164 site-specific estimates of ACSP. Most study sites are located in the contiguous United States (n = 137; fig. S1A), with others in Europe (fig. S1B), Iceland, Costa Rica, Panama, Chile, and New Zealand (sites not shown in fig. S1). Complete citation information for all sites retained in this study are listed in data file S1. Before analyses, all ACSP estimates were standardized to units of milligrams AFDM per square meter per year (mg AFDM m⁻² year⁻¹), using conversion factors by Waters (81), and then natural log-transformed to improve normality.

Environmental covariates

To test the hypothesized relationships shown in the metamodel (Fig. 1), we appended a suite of environmental covariates, as well as author-reported total invertebrate biomass and density estimates, to each of the 164 ACSP study sites. These covariates included location information (longitude and latitude), water quality parameters (e.g., water temperature, pH, and conductivity), physical habitat characteristics (e.g., stream channel dimensions and substrate particle size), and climate conditions (air temperature and precipitation). Whenever possible, covariate values were obtained from the original literature sources or from companion studies that were conducted at the same study sites. Complete descriptions of all covariates in the ACSP database are listed in table S1 and detailed methods used to obtain them are provided in the Supplementary Materials. Availability of covariate data was variable, with many more covariates accessible for U.S. sites than non-U.S. sites. Two versions of the ACSP database were therefore prepared: a U.S.-only database with a large selection of covariates for each of the 137 U.S. sites (see data file S2) and a global-scale database inclusive of all 164 study sites but with a limited number of covariates for each site (see data file S3). Many of the covariates in the U.S. database were not represented in the metamodel (Fig. 1); these were included in the compiled database to provide a ready data source for testing hypotheses not considered here.

Hydrologic modeling

Hydrologic indices were independently predicted for each U.S. site, using time series of daily discharge records from the U.S. Geological Survey (USGS) Water Services portal (https://waterservices.usgs.gov), and appended to the ACSP dataset. We began by selecting a national sample of flow gauges from the USGS Geospatial Attributes of Gages for Evaluating Streamflow database [GAGES II; Falcone *et al.* (82)] that featured (nearly) continuous discharge records from 1970 through the present day; this duration allowed robust characterization of contemporary flow dynamics while maximizing the number and spatial distribution of gauges used to develop hydrologic models. We then removed gauges with upstream impoundments of >50 Ml (megaliters) km⁻² (impoundment volume scaled by watershed area), as these sites may be more strongly influenced by dam release operations than natural precipitation and land-use factors (83). This screening process resulted in a sample of 2568 gauges.

Random forest models were then developed for a set of hydrologic indices, incorporating four of five hydrologic components: flow magnitude, frequency, duration, and rate of change (84). We began with models of 12 hydrologic indices that are broadly representative of perennial streams in a variety of conditions (85, 86). Flow magnitude was characterized by variability, skewness, two measures of spread, and median annual maximum flow. Flow frequency was characterized by low flow pulse percentage, frequency of low flow events, and two measures of high flood pulse percentage. Flow duration was characterized by the 30-day minimum and maximum daily discharge. Rate of change was characterized by hydrologic flashiness (87). Following Carlisle et al. (88), random forest models (500 iterations per model) were built for each flow index using the randomForest library in R (89). Each random forest model was parameterized with a suite of predictor variables representing precipitation, underlying geology, and land use, but excluding predictor variables that were subsequently used in SEMs of secondary production (forest cover, watershed size, and impervious surface in the upstream watershed). Random forest model fit differed among hydrologic indices, and we focused on those models that explained \geq 45% of the variance in their respective indices. These included flashiness, high flow pulse percentage (i.e., number of daily values within a time series) exceeding the daily median by ×7 (HighFlowPulse7) and ×3 margins (HighFlowPulse3), minimum consecutive 30-day flow, low flow pulse percentage, and variation in daily flow. The final six random forest models were then used to predict flow indices at each of the stream sites included in the U.S.ACSP database.

Data analyses

A subset of 13 covariates (see Table 1), each representative of a hypothesized ACSP driver as shown in Fig. 1, was first selected for univariate regression analyses of U.S. streams. Associations between these covariates and ACSP were then independently tested with regression models of the general form ACSP = $b \times C + Y$, where C is the covariate of interest, b is a coefficient (i.e., regression model slope) relating C to ACSP, and Y is an intercept term. Natural log transformations were used to improve normality for covariates with skewed distributions. In cases where C was a categorical variable (e.g., stream order), b was calculated for each categorical level in comparison to a baseline level. For example, the stream order baseline was first-order (i.e., the smallest) streams. Thus, b for second-order streams was the difference between first- and second-order streams.

Because measurement units differed among covariates, standardized regression model parameter estimates were calculated [β (90)] to facilitate direct comparisons among covariates. Coefficients of determination (r^2) were also calculated for each regression model to estimate the variation in ACSP explained by the respective covariate.

Next, SEM was used to confront the ACSP metamodel (Fig. 1) with the empirical ACSP and covariate data (table S1). This allowed us to (i) assess the complete graphical network of hypothesized interactions and relationships, with the directions of links (i.e., paths) in the SEM diagram indicating causal influences, and (ii) test the overall fit of the network (31, 91). Separate models were fit to the U.S. and global databases, with the former used to test the complete network of interrelationships among covariates shown in Fig. 1 and the latter testing for generality of the U.S. results at the global scale. At each of the two scales, an iterative process of testing and linking covariates, consistent with the hypotheses outlined in the metamodel, was used to produce a final SEM of ACSP. Three indices of model fit were used with conventional significance thresholds—the $\chi^2 P$ value $(\chi^2 P > 0.05)$, the standardized root mean squared residual (SRMR \leq 0.08), and the comparative fit index (CFI \geq 0.95)—to assess the overall fit of each SEM (92). All SEM procedures were conducted with the lavaan library in R (93). Code to build the final U.S. and global models is provided in data file S4.

SUPPLEMENTARY MATERIALS

Supplementary material for this article is available at http://advances.sciencemag.org/cgi/content/full/5/4/eaav2348/DC1

Supplementary Materials and Methods

Fig. S1. Maps of study sites included in the ACSP database.

Table S1. Data dictionary for variables included in the secondary production database for U.S. streams.

Data file S1. Citation records for all studies included in the ACSP database.

Data file S2. Complete secondary production and covariate data for all U.S. streams.

Data file S3. Secondary production and covariate data for the global streams database.

Data file S4. R code to build the U.S and global SEM models.

References (98-102)

REFERENCES AND NOTES

- A. D. Huryn, J. B. Wallace, Life history and production of stream insects. Annu. Rev. Entomol. 45. 83–110 (2000).
- R. O. Hall Jr., J. B. Wallace, S. L. Eggert, Organic matter flow in stream food webs with reduced detrital resource base. *Ecology* 81, 3445–3463 (2000).
- A. C. Benke, J. B. Wallace, High secondary production in a Coastal Plain river is dominated by snag invertebrates and fuelled mainly by amorphous detritus. Freshw. Biol. 60, 236–255 (2015)
- G. Woodward, D. C. Speirs, A. G. Hildrew, Quantification and resolution of a complex, size-structured food web. Adv. Ecol. Res. 36, 85–135 (2005).
- W. F. Cross, C. V. Baxter, E. J. Rosi-Marshall, R. O. Hall Jr., T. A. Kennedy, K. C. Donner, H. A. Wellard Kelly, S. E. Z. Seegert, K. E. Behn, M. D. Yard, Food-web dynamics in a large river discontinuum. *Ecol. Monogr.* 83, 311–337 (2013).
- D. P. Whiting, M. R. Whiles, M. L. Stone, Patterns of macroinvertebrate production, trophic structure, and energy flow along a tallgrass prairie stream continuum. *Limnol. Oceanogr.* 56, 887–898 (2011)
- M. R. Whiles, J. B. Wallace, Macroinvertebrate production in a headwater stream during recovery from anthropogenic disturbance and hydrologic extremes. Can. J. Fish. Aq. Sci. 52, 2402–2422 (1995).
- D. M. Carlisle, W. H. Clements, Growth and secondary production of aquatic insects along a gradient of Zn contamination in Rocky Mountain streams. J. N. Am. Benthol. Soc. 22, 582–597 (2003).
- N. S. Ismail, C. E. Müller, R. R. Morgan, R. G. Luthy, Uptake of contaminants of emerging concern by the bivalves *Anodonta californiensis* and *Corbicula fluminea*. *Environ. Sci. Technol.* 48, 9211–9219 (2014).
- National Research Council, Ecosystem services of bivalves: Implications for restoration, in *Ecosystem Concepts for Sustainable Bivalve Mariculture* (National Academies Press, 2010), pp. 123–132.

SCIENCE ADVANCES | RESEARCH ARTICLE

- E. Mortensen, J. L. Simonsen, Production estimates of the benthic invertebrate community in a small Danish stream. *Hydrobiologia* 102, 155–162 (1983).
- M. A. Wilzbach, K. W. Cummins, J. D. Hall, Influence of habitat manipulations on interactions between cutthroat trout and invertebrate drift. *Ecology* 67, 898–911 (1986)
- A. D. Huryn, Growth and voltinism of lotic midge larvae: Patterns across an Appalachian Mountain basin. *Limnol. Oceanogr.* 35, 339–351 (1990).
- A. D. Huryn, A. C. Benke, G. M. Ward, Direct and indirect effects of geology on the distribution, biomass, and production of the freshwater snail *Elimia. J. N. Am. Benthol. Soc.* 14. 519–534 (1995).
- A. Morin, P. Dumont, A simple model to estimate growth rate of lotic insect larvae and its value for estimating population and community production. J. N. Am. Benthol. Soc. 13, 357–367 (1994).
- D. Nelson, J. P. Benstead, A. D. Huryn, W. F. Cross, J. M. Hood, P. W. Johnson, J. R. Junker, G. M. Gíslason, J. S. Ólafsson, Shifts in community size structure drive temperature invariance of secondary production in a stream-warming experiment. *Ecology* 98, 1797–1806 (2017).
- A. C. Benke, A. D. Huryn, Secondary production and quantitative food webs, in Stream Ecology. Volume 2: Ecosystem Function (Elsevier, ed. 3, 2017), pp. 235–254.
- A. P. Covich, M. A. Palmer, T. A. Crowl, The role of benthic invertebrate species in freshwater ecosystems: Zoobenthic species influence energy flows and nutrient cycling. *Bioscience* 49, 119–127 (1999).
- D. Nelson, J. P. Benstead, A. D. Huryn, W. F. Cross, J. M. Hood, P. W. Johnson, J. R. Junker, G. M. Gíslason, J. S. Ólafsson, Experimental whole-stream warming alters community size structure. *Glob. Chana. Biol.* 23, 2618–2628 (2017).
- A. C. Benke, M. R. Whiles, Life table vs secondary production analyses—Relationships and usage in ecology. J. N. Am. Benthol. Soc. 30, 1024–1032 (2011).
- A. C. Benke, Secondary production as part of bioenergetic theory—Contributions from freshwater benthic science. River Res. Appl. 26, 36–44 (2010).
- C. Segura, P. Caldwell, G. Sun, S. McNulty, Y. Zhang, A model to predict stream water temperature across the conterminous USA. *Hydrol. Process.* 29, 2178–2195 (2015).
- P. J. Mulholland, C. S. Fellows, J. L. Tank, N. B. Grimm, J. R. Webster, S. K. Hamilton, E. Martí, L. Ashkenas, W. B. Bowden, W. K. Dodds, W. H. Mcdowell, M. J. Paul, B. J. Peterson, Inter-biome comparison of factors controlling stream metabolism. *Freshw. Biol.* 46, 1503–1517 (2001).
- B. O. L. Demars, J. R. Manson, J. S. Ólafsson, G. M. Gíslason, R. Gudmundsdóttir, G. Woodward, J. Reiss, D. E. Pichler, J. J. Rasmussen, N. Friberg, Temperature and the metabolic balance of streams. *Freshw. Biol.* 56, 1106–1121 (2011).
- E. R. Hannesdóttir, G. M. Gíslason, J. S. Ólafsson, Ó. P. Ólafsson, E. J. O'Gorman, Increased stream productivity with warming supports higher trophic levels. Adv. Ecol. Res. 48, 285–342 (2013).
- N. B. Grimm, S. G. Fisher, Stability of periphyton and macroinvertebrates to disturbance by flash floods in a desert stream. J. N. Am. Benthol. Soc. 8, 293–307 (1989).
- R. G. Death, The effect of habitat stability on benthic invertebrate communities:
 The utility of species abundance distributions. Hydrobiologia 317, 97–107 (1996).
- I. G. Jowett, Hydraulic constraints on habitat suitability for benthic invertebrates in gravel-bed rivers. River Res. Appl. 19, 495–507 (2003).
- P. D. Markos, M. D. Kaller, W. E. Kelso, Channel stability and the structure of coastal stream aquatic insect assemblages. Fundam. Appl. Limnol. 188, 187–199 (2016).
- J. B. Grace, D. R. Schoolmaster Jr., G. R. Guntenspergen, A. M. Little, B. R. Mitchell, K. M. Miller, E. W. Schweiger, Guidelines for a graph-theoretic implementation of structural equation modeling. *Ecosphere* 3, 1–44 (2012).
- J. B. Grace, Structural Equation Modeling and Natural Systems (Cambridge Univ. Press, Cambridge, 2006).
- A. C. Benke, Concepts and patterns of invertebrate production in running waters. Verb. Int. Ver. Theor. Angew. Limnol. 25, 15–38 (1993).
- L. R. Harrison, C. J. Legleiter, M. A. Wydzga, T. Dunne, Channel dynamics and habitat development in a meandering, gravel bed river. Water Resour. Res. 47, W04513 (2011).
- K. M. Potter, F. W. Cubbage, R. H. Schaberg, Multiple-scale landscape predictors of benthic macroinvertebrate community structure in North Carolina. *Landscape Urban Plann.* 71, 77–90 (2005).
- J. C. Rutherford, S. Blackett, C. Blackett, L. Saito, R. J. Davies-Colley, Predicting the effects of shade on water temperature in small streams. N. Z. J. Mar. Freshwat. Res. 31, 707–721 (1997).
- 36. D. Caissie, The thermal regime of rivers: A review. Freshw. Biol. 51, 1389-1406 (2006).
- J. C. Morrill, R. C. Bales, M. H. Conklin, Estimating stream temperature from air temperature: Implications for future water quality. *J. Environ. Eng.* 131, 139–146 (2005).
- L. L. Larry, L. L. Shane, Riparian shade and stream temperature: A perspective. Rangelands 18, 149–152 (1996).
- G. C. Poole, C. H. Berman, An ecological perspective on in-stream temperature: Natural heat dynamics and mechanisms of human-caused thermal degradation. *Environ. Manag.* 27, 787–802 (2001).

- M. A. Rahman, A. Moser, T. Rötzer, S. Pauleit, Within canopy temperature differences and cooling ability of *Tilia cordata* trees grown in urban conditions. *Build. Environ.* 114, 118–128 (2017)
- J. H. Brown, J. F. Gillooly, A. P. Allen, V. M. Savage, G. B. West, Toward a metabolic theory of ecology. *Ecology* 85, 1771–1789 (2004).
- C. B. Field, M. J. Behrenfeld, J. T. Randerson, P. Falkowski, Primary production of the biosphere: Integrating terrestrial and oceanic components. Science 281, 237–240 (1998).
- J. S. Richardson, Seasonal food limitation of detritivores in a montane stream: An experimental test. *Ecology* 72, 873–887 (1991).
- B. J. Peterson, L. Deegan, J. Helfrich, J. E. Hobbie, M. Hullar, B. Moller, T. E. Ford, A. Hershey, A. Hiltner, G. Kipphut, M. A. Lock, D. M. Fiebig, V. McKinley, M. C. Miller, J. R. Vestal, R. Ventullo, G. Volk, Biological responses of a tundra river to fertilization. *Ecology* 74, 653–672 (1993).
- J. B. Wallace, S. L. Eggert, J. L. Meyer, J. R. Webster, Effects of resource limitation on a detrital-based ecosystem. *Ecol. Monogr.* 69, 409–442 (1999).
- T. M. Iversen, Ingestion and growth in Sericostoma personatum (Trichoptera) in relation to the nitrogen content of ingested leaves. Oikos 25, 278–282 (1974).
- G. M. Ward, K. W. Cummins, Effects of food quality on growth of a stream detritivore, Paratendipes Albimanus (Meigen) (Diptera: Chironomidae). Ecology 60, 57–64 (1979).
- C. L. Fuller, M. A. Evans-White, S. A. Entrekin, Growth and stoichiometry of a common aquatic detritivore respond to changes in resource stoichiometry. *Oecologia* 177, 837–848 (2015).
- W. F. Cross, J. B. Wallace, A. D. Rosemond, S. L. Eggert, Whole-system nutrient enrichment increases secondary production in a detritus-based ecosystem. *Ecology* 87, 1556–1565 (2006).
- J. B. Wallace, S. L. Eggert, J. L. Meyer, J. R. Webster, Multiple trophic levels of a forest stream linked to terrestrial litter inputs. Science 277, 102–104 (1997).
- W. K. Dodds, Eutrophication and trophic state in rivers and streams. Limnol. Oceanogr. 51, 671–680 (2006).
- 52. F. Woodward, Climate and Plant Distribution (Cambridge Univ. Press, 1987).
- A. Hoffman, P. Parsons, Extreme Environmental Change and Evolution (Cambridge Univ. Press, 1997).
- P. B. Reich, J. Oleksyn, Global patterns of plant leaf N and P in relation to temperature and latitude. Proc. Natl. Acad. Sci. U.S.A. 101, 11001–11006 (2004).
- W. K. Dodds, K. Gido, M. R. Whiles, M. D. Daniels, B. P. Grudzinski, The stream biome gradient concept: Factors controlling lotic systems across broad biogeographic scales. *Freshw. Sci.* 34, 1–19 (2015).
- B. Bond-Lamberty, S. D. Peckham, D. E. Ahl, S. T. Gower, Fire as the dominant driver of central Canadian boreal forest carbon balance. *Nature* 450, 89–92 (2007).
- 57. M. Zhao, S. W. Running, Drought-induced reduction in global terrestrial net primary production from 2000 through 2009. *Science* **329**, 940–943 (2010).
- M. Piniewski, C. Prudhomme, M. C. Acreman, L. Tylec, P. Oglęcki, T. Okruszko, Responses of fish and invertebrates to floods and droughts in Europe. *Ecohydrology* 10, e1793 (2017).
- J. Jackson, S. G. Fisher, Secondary production, emergence, and export of aquatic insects of a Sonoran Desert stream. *Ecology* 67, 629–638 (1986).
- J. E. Gladden, L. A. Smock, Macroinvertebrate distribution and production on the floodplains of two lowland headwater streams. Freshw. Biol. 24, 533–545 (1990).
- R. O. Hall Jr., M. F. Dybdahl, M. C. VanderLoop, Extremely high secondary production of introduced snails in rivers. Ecol. Appl. 16, 1121–1131 (2006).
- M. A. Chadwick, A. D. Huryn, Role of habitat in determining macroinvertebrate production in an intermittent-stream system. Freshw. Biol. 52, 240–251 (2007).
- M. E. Ledger, F. K. Edwards, L. E. Brown, A. M. Milner, G. Woodward, Impact of simulated drought on ecosystem biomass production: An experimental test in stream mesocosms. *Glob. Chang. Biol.* 17, 2288–2297 (2011).
- N. Majdi, B. Mialet, S. Boyer, M. Tackx, J. Leflaive, S. Boulêtreau, L. Ten-Hage, F. Julien, R. Fernandez, E. Buffan-Dubau, The relationship between epilithic biofilm stability and its associated meiofauna under two patterns of flood disturbance. Freshw. Sci. 31, 38–50 (2012).
- S. G. Fisher, L. J. Gray, N. B. Grimm, D. E. Busch, Temporal succession in a desert stream ecosystem following flash flooding. *Ecol. Monogr.* 52, 93–110 (1982).
- G. G. Mittelbach, C. F. Steiner, S. M. Scheiner, K. L. Gross, H. L. Reynolds, R. B. Waide, M. R. Willig, S. I. Dodson, L. Gough, What is the observed relationship between species richness and productivity? *Ecology* 82, 2381–2396 (2001).
- B. J. Cardinale, D. S. Srivastava, J. Emmett Duffy, J. P. Wright, A. L. Downing, M. Sankaran,
 C. Jouseau, Effects of biodiversity on the functioning of trophic groups and ecosystems.
 Nature 443, 989–992 (2006).
- B. Statzner, V. H. Resh, Multiple-site and-year analyses of stream insect emergence: A test of ecological theory. *Oecologia* 96, 65–79 (1993).
- M. R. Whiles, B. S. Goldowitz, Hydrologic influences on insect emergence production from Central Platte River WETLANDS. Ecol. Appl. 11, 1829–1842 (2001).
- M. R. Vinson, C. P. Hawkins, Broad-scale geographical patterns in local stream insect genera richness. *Ecography* 26, 751–767 (2003).

SCIENCE ADVANCES | RESEARCH ARTICLE

- L. A. Bêche, B. Statzner, Richness gradients of stream invertebrates across the USA: Taxonomy- and trait-based approaches. *Biodivers. Conserv.* 18, 3909–3930 (2009).
- J. C. Finlay, Stream size and human influences on ecosystem production in river networks. Ecosphere 2. 1–21 (2011).
- Intergovernmental Panel on Climate Change, "AR5 synthesis report: Climate change 2014" (Technical Report, 2014).
- R. Allen, B. Soden, Atmospheric warming and the amplification of precipitation extremes. Science 321, 1481–1484 (2008).
- R. Seager, M. Ting, C. Li, N. Naik, B. Cook, J. Nakamura, H. Liu, Projections of declining surface-water availability for the southwestern United States. *Nat. Clim. Chang.* 3, 482–486 (2013)
- R. Seager, M. Ting, I. Held, Y. Kushnir, J. Lu, G. Vecchi, H. P. Huang, N. Harnik, A. Leetmaa, N. C. Lau, C. Li, J. Velez, N. Naik, Model projections of an imminent transition to a more arid climate in southwestern North America. Science 316, 1181–1184 (2007).
- A. Dai, Increasing drought under global warming in observations and models. Nat. Clim. Chana. 3, 52–58 (2013).
- N. L. Poff, J. D. Olden, N. K. M. Vieira, D. S. Finn, M. P. Simmons, B. C. Kondratieff, Functional trait niches of North American lotic insects: Traits-based ecological applications in light of phylogenetic relationships. J. N. Am. Benthol. Soc. 25, 730–755 (2006).
- J. C. White, D. M. Hannah, A. House, S. J. V. Beatson, A. Martin, P. J. Wood, Macroinvertebrate responses to flow and stream temperature variability across regulated and non-regulated rivers. *Ecohydrology* 10, e1773 (2017).
- 80. D. G. Jenkins, Estimating ecological production from biomass. Ecosphere 6, 1–31 (2015).
- 81. T. F. Waters, Secondary production in inland waters. Adv. Ecol. Res. 10, 91-164 (1977).
- J. A. Falcone, D. M. Carlisle, D. M. Wolock, M. R. Meador, GAGES: A stream gage database for evaluating natural and altered flow conditions in the conterminous United States. *Ecology* 91, 621 (2010).
- 83. L. L. Yuan, Using correlation of daily flows to identify index gauges for ungauged streams. *Water Resour. Res.* **49**, 604–613 (2013).
- N. L. Poff, J. D. Allan, M. B. Bain, J. R. Karr, K. L. Prestegaard, B. D. Richter, R. E. Sparks, J. C. Stromberg, The natural flow regime. *Bioscience* 47, 769–784 (1997).
- J. D. Olden, N. L. Poff, Redundancy and the choice of hydrologic indices for characterizing streamflow regimes. *River Res. Appl.* 19, 101–121 (2003).
- C. J. Patrick, L. L. Yuan, Modeled hydrologic metrics show links between hydrology and the functional composition of stream assemblages. *Ecol. Appl.* 27, 1605–1617 (2017).
- 87. D. B. Baker, R. P. Richards, T. T. Loftus, J. W. Kramer, A new flashiness index: Characteristics and applications to midwestern rivers and streams. *J. Am. Water Resour. Assoc.* **40**,
- D. M. Carlisle, D. M. Wolock, M. R. Meador, Alteration of streamflow magnitudes and potential ecological consequences: A multiregional assessment. Front. Ecol. Environ. 9, 264–270 (2010).
- D. R. Cutler, T. C. Edwards Jr., K. H. Beard, A. Cutler, K. T. Hess, J. Gibson, J. J. Lawler, Random forests for classification in ecology. *Ecology* 88, 2783–2792 (2007).
- 90. J. R. Hair, R. C. Anderson, R. Tatham, W. Black, Multivariate Data Analysis (Prentice Hall, ed. 5, 1998).
- 91. B. Shipley, Cause and Correlation in Biology: A User's Guide to Path Analysis, Structural Equations and Causal Inference (Cambridge Univ. Press, 2002).
- L. Hu, P. M. Bentler, Cutoff criteria for fit indexes in covariance structure analysis: Conventional criteria versus new alternatives. Struct. Equ. Modeling 6, 1–55 (1999).
- 93. Y. Rosseel, lavaan: An R Package for structural equation modeling. J. Stat. Softw. 48 (2012).
- 94. N. J. Hetrick, M. A. Brusven, W. R. Meehan, T. C. Bjornn, Changes in solar input, water temperature, periphyton accumulation, and allochthonous input and storage after

- canopy removal along two small salmon streams in southeast Alaska. *Trans. Am. Fish. Soc.* **127.** 859–875 (1998).
- O. Mohseni, T. R. Erickson, H. G. Stefan, Upper bounds for stream temperatures in the contiguous United States. J. Environ. Eng. 128, 4–11 (2002).
- R. L. Vannote, G. W. Minshall, K. W. Cummins, J. R. Sedell, C. E. Cushing, The river continuum concept. Can. J. Fish. Aquat. Sci. 37, 130–137 (1980).
- M. Diana, J. D. Allan, D. Infante, The influence of physical habitat and land use on stream fish assemblages in southeastern Michigan. Am. Fish. Soc. Symp. 48, 359–374 (2006).
- L. McKay, T. Bondelid, T. Dewald, A. Rea, C. Johnston, R. Moore, NHDPlus Version 2: User Guide (Data Model Version 2.1) (Horizon Systems, 2015).
- R. A. Hill, M. H. Weber, S. G. Leibowitz, A. R. Olsen, D. J. Thornbrugh, The Stream-Catchment (StreamCat) dataset: A database of watershed metrics for the conterminous United States. J. Am. Water Resour. Assoc. 52, 120–128 (2016).
- 100. L. Breiman, Random forests. Mach. Learn. 45, 5-32 (2001).
- D. M. Carlisle, J. Falcone, D. M. Wolock, M. R. Meador, R. H. Norris, Predicting the natural flow regime: Models for assessing hydrological alteration in streams. *River Res. Appl.* 26, 118–136 (2010).
- C. K. Wentworth, A scale of grade and class terms for clastic sediments. J. Geol. 30, 377–392 (1922).

Acknowledgments

Funding: We thank the U.S. NSF (grant no. DEB-1354867) for funding the Stream Resiliency Research Coordination Network (RCN) and the National Center for Ecological Analysis and Synthesis (NCEAS) for hosting the Structural Equation and Mechanistic Modeling Working Group, where many of these ideas were developed. C.J.P. received additional support from the National Academy of Science, Engineering, and Medicine (GRP-ECRF). D.J.M. received additional support through the NSF (DEB-1553111). G.W. was supported by the UK Natural Environment Research Council Large Grant (NE/M020843/1). W.F.C. received additional support through the NSF (DEB-0949774). Graphic icons used in Figs. 1 and 2 were downloaded from Freepik (www.freepik.com) and the Integration and Application Network, University of Maryland Center for Environmental Science (ian.umces.edu/imagelibrary/). Author contributions: All authors contributed to the development of the dataset used in these analyses and writing and editing of the manuscript and supplementary documents. C.J.P. was responsible for the hydrologic modeling. D.J.M. was responsible for the geospatial analyses. C.J.P., D.J.M., and J.H.L. were responsible for the statistical analyses. Competing interests: The authors declare that they have no competing interests. Data and materials availability: All data needed to evaluate the conclusions in the paper are present in the paper and/or the Supplementary Materials. Additional data related to this paper may be requested from the authors.

Submitted 28 August 2018 Accepted 27 February 2019 Published 17 April 2019 10.1126/sciadv.aav2348

Citation: C. J. Patrick, D. J. McGarvey, J. H. Larson, W. F. Cross, D. C. Allen, A. C. Benke, T. Brey, A. D. Huryn, J. Jones, C. A. Murphy, C. Ruffing, P. Saffarinia, M. R. Whiles, J. B. Wallace, G. Woodward, Precipitation and temperature drive continental-scale patterns in stream invertebrate production. *Sci. Adv.* 5, eaav2348 (2019).



advances.sciencemag.org/cgi/content/full/5/4/eaav2348/DC1

Supplementary Materials for

Precipitation and temperature drive continental-scale patterns in stream invertebrate production

C. J. Patrick*, D. J. McGarvey, J. H. Larson, W. F. Cross, D. C. Allen, A. C. Benke, T. Brey, A. D. Huryn, J. Jones, C. A. Murphy, C. Ruffing, P. Saffarinia, M. R. Whiles, J. B. Wallace, G. Woodward

*Corresponding author. Email: christopher.patrick@tamucc.edu

Published 17 April 2019, *Sci. Adv.* **5**, eaav2348 (2019) DOI: 10.1126/sciadv.aav2348

The PDF file includes:

Supplementary Materials and Methods

Fig. S1. Maps of study sites included in the ACSP database.

Table S1. Data dictionary for variables included in the secondary production database for U.S. streams.

References (98–102)

Other Supplementary Material for this manuscript includes the following:

(available at advances.sciencemag.org/cgi/content/full/5/4/eaav2348/DC1)

Data file S1 (.csv format). Citation records for all studies included in the ACSP database.

Data file S2 (.csv format). Complete secondary production and covariate data for all U.S. streams.

Data file S3 (.csv format). Secondary production and covariate data for the global streams database.

Data file S4 (.txt format). R code to build the U.S and global SEM models.

Supplementary Materials and Methods

U.S. Database – Landscape and Climate Attributes

Annual community secondary production (ACSP) and attribute data from all sample sites within the U.S., as reported by the original authors (see Data file S1), were appended with additional environmental covariates using a geographic information system (GIS) to superimpose sample locations on their corresponding digital stream segments from the 1:100,000 scale National Hydrography Dataset (NHD) version 2 (98). Locations of all U.S. sample points (originally reported longitude and latitude coordinates) were manually verified or adjusted in the GIS to maximize spatial accuracy and consistency among all data sources. Local stream channel slope, Strahler stream order, and the summed length of all upstream stream segments (relative to a given sample location; the 'ArbolateSum') were appended directly from the NHD attribute tables. Elevation, basin area, and mean annual runoff were obtained for each sample location from the StreamCat database (99) at both basin (i.e., the complete drainage basin, relative to a given NHD stream segment, when delineated from the downstream end of that segment) and catchment scales (i.e., the fraction of the drainage basin, relative to a given NHD segment, that is immediately lateral to the segment but exclusive of all area upstream of the upper end of that segment). An additional 95 covariates from the StreamCat database, representing a variety of anthropogenic, geologic, and land cover factors, were also appended at basin and catchment scales (see Table S1). Finally, we used WorldClim (www.worldclim.org) records to append the 19 'bioclimate' variables, representing mean annual and mean monthly air temperature and precipitation, to the U.S. ACSP dataset. All StreamCat and WorldClim data were queried and matched to the U.S. sample sites using the master cataloging codes (COMID values) from the NHD database. All spatial procedures were implemented in ESRI ArcMap 10.2 software (Environmental Systems Research Institute, Redlands, California). StreamCat variables that were originally expressed as percentages were arcsine square root transformed. All other covariates except StreamOrder were strongly skewed and therefore natural log transformed. Scaling adjustments were made as needed to prevent transformation errors for zero-value observations. Units, transformations, and scaling adjustments are listed for all covariates in Table S1.

U.S. Database – Hydrologic and Sediment Indices

Hydrologic indices were independently predicted for each U.S. site, using time-series of daily discharge records from the U.S. Geological Survey (USGS) Water Services portal (https://waterservices.usgs.gov), and appended to the U.S. ACSP dataset. We began by selecting a national sample of flow gauges from the USGS Geospatial Attributes of Gages for Evaluating Streamflow database (82) that featured nearly continuous discharge records from 1970 through the present; this duration allowed for robust characterization of contemporary flow dynamics while maximizing the number and spatial distribution of gauges used to development hydrologic models. We then removed gauges with upstream impoundments > 50 ML/km² (impoundment volume scaled by basin area), as these sites may be more strongly influenced by dam release operations than natural precipitation and land use factors (83). This screening process resulted in a flow database that included 2568 gauges.

Random forest models (100) were then used to predict a series of hydrologic indices, representing four of the five flow regime components: magnitude, frequency, duration, and rate of change (84). We began with models of 12 hydrologic indices that are broadly representative of perennial streams in a variety of conditions (85, 86). Flow magnitude was characterized by variability, skewness, two measures of spread, and median annual maximum flow. Flow frequency was characterized by low flow pulse percentage, frequency of low flow events, and two measures of high flood pulse percentage. Flow duration was characterized by the 30-day minimum and maximum daily discharge. Rate of change was characterized by hydrologic flashiness (87). Following Carlisle et al. (101), random forest models (500 iterations per model) were built for each flow index using the randomForest library in R (89). Each random forest model was parameterized with a suite of predictor variables representing precipitation, underlying geology, and land use, but excluding predictor variables that were subsequently used in structural equation models of ACSP (forest cover, basin size, and impervious surface in the upstream basin). Model fit differed among hydrologic indices and we focused on those models that explained \geq 45% of the variance in their respective indices. These included flashiness, high flow pulse percentage (i.e., number of daily values within a time-series) exceeding the daily median by ×7 ('HighFlowPulse7') and ×3 margins ('HighFlowPulse3'), minimum consecutive 30-day flow, low flow pulse percentage, and variation in daily flow (see r^2 values in Table S1). The final six random forest models were then used to predict flow indices at each of the stream sites included in the U.S. database.

Two sediment variables were also derived from empirical field data and appended to the site attributes. Original sources most often reported a single, dominant substrate type or proportions within 3-5 size categories (e.g., boulder, cobble, sand, etc.). We converted these descriptive categories to average grain sizes (diameter in mm) using the Wentworth scale (102). When proportions by size were reported, we then calculated weighted average sediment size ('SedimentHierarchical'). Otherwise, we used the reported dominant grain size or un-weighted average of all reported size categories ('SedimentAverage').

Global Database

Because, the NHD and StreamCat attributes were not available for non-U.S. sites, the number of global covariates was necessarily smaller (see Data file S3). Each site in the global ACSP database was appended with 16 covariates, most of which were obtained directly from the original publications. Mean catchment elevation ('ElevationCatch') was interpolated for non-U.S. sites from a 2.5' digital elevation model, downloaded from WorldClim. Mean annual air temperature ('Bioclimate1') and mean annual precipitation ('Bioclimate12') were also interpolated from WorldClim records. All covariate units, transformations, and scaling adjustments in the global database are consistent with definitions in Table S1.

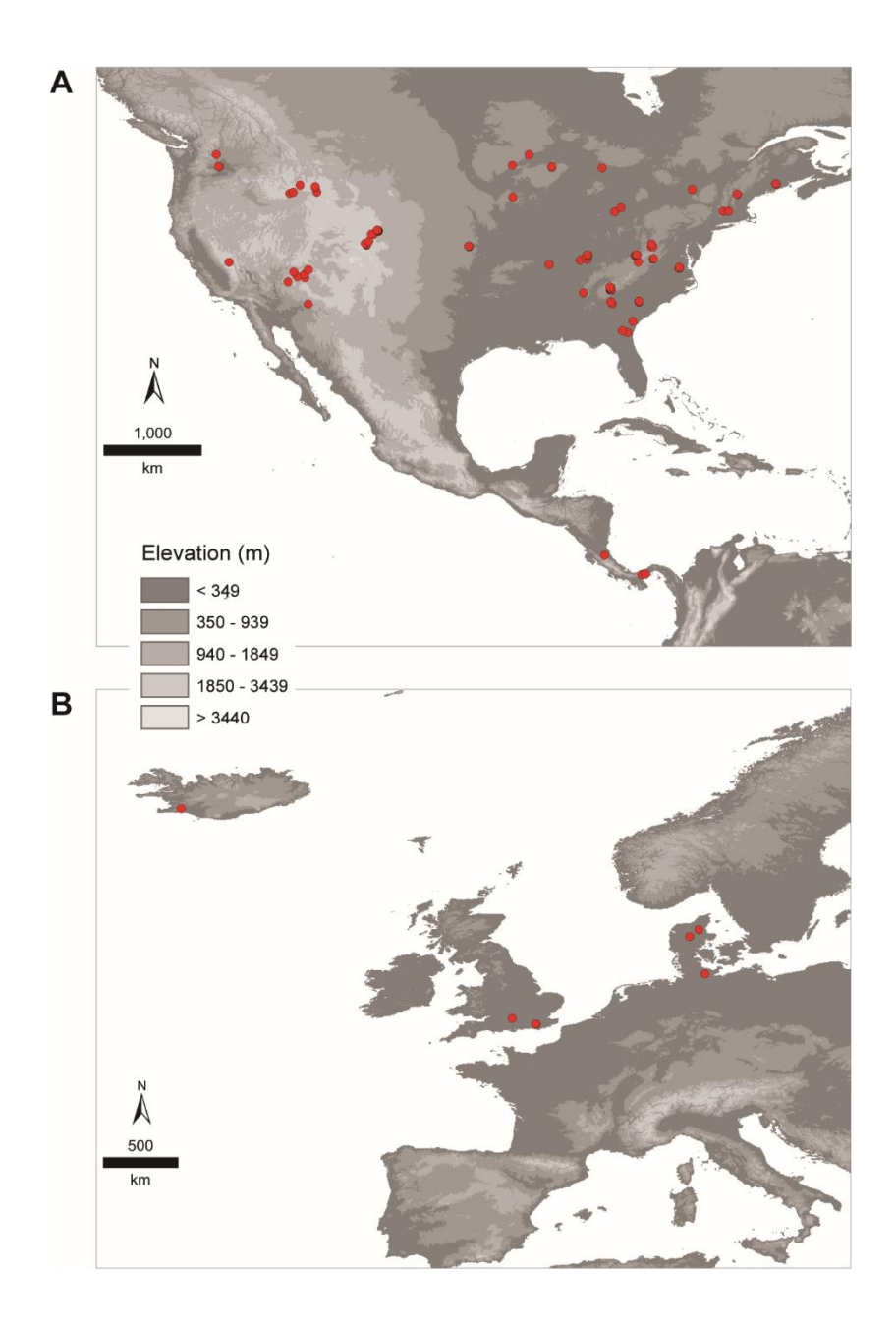


Fig. S1. Maps of study sites included in the ACSP database. Most reported studies were from streams and rivers in the U.S. (panel A), with fewer studies in Central America (panel A), Iceland and northern Europe (panel B). One site was included from Chile and three sites from New Zealand (not shown in maps). Other regions of the globe are not shown here, as ACSP studies have not been reported from them. Note that the continental-scale maps obscure the locations of some sites in close spatial proximity.

Table S1. Data dictionary for variables included in the secondary production database for U.S. streams. Records include basic descriptions of each variable with units of measurement, data sources, and data transformations that were used prior to structural equation modeling. All natural log transformations included the addition of a non-zero scaling adjustment (Natural log = $\ln(\text{variable} + 0.0000001)$; Natural log (+121) = $\ln(\text{variable} + 121)$; Natural log (+200) = $\ln(\text{variable} + 200)$.

Variable	Description	Source	Transformation
Index	Unique sample identifier.	n/a	n/a
SiteID	Unique label used to identify each sample in the database (concatenation of authors, publication date, and stream/site identifiers).	n/a	n/a
Production	Community-level annual secondary production, in milligrams per square meter per year (ash-free dry mass).	Field data (see original citation)	Natural log
Biomass	Total biomass density, in milligrams per square meter (ash-free dry mass).	Field data (see original citation)	Natural log
Density	Density of individuals sampled as mean abundance per square meter.	Field data (see original citation)	Natural log
Discharge	Mean annual discharge, in liters per second.	Field data (see original citation)	Natural log
ChannelWidth	Mean wetted channel width, in meters.	Field data (see original citation)	Natural log
WaterTemperature	Mean annual water temperature, in degrees Celsius.	Field data (see original citation)	Natural log
pH	Mean pH.	Field data (see original citation)	Natural log
Conductivity	Mean conductivity, in microsiemens per centimeter.	Field data (see original citation)	Natural log
СРОМ	Coarse particulate organic matter, in grams per square meter (ash-free dry mass).	Field data (see original citation)	Natural log
Longitude	Longitude of the study site, in decimal degrees.	Interpolated in GIS	Natural log (x + 121)
Latitude	Absolute latitude of the study site, in decimal degrees.	Interpolated in GIS	Natural log
ElevationCatch	Mean elevation within the catchment of a focal stream segment, in meters above sea level.	StreamCat ^a	Natural log
ElevationWater	Mean elevation within the watershed contributing to a focal stream segment, in meters above sea level.	StreamCat ^a	Natural log
Slope	Slope of the focal stream segment in dimensionless units (rise in meters over run in meters).	NHD Plus Version 2 ^b	Natural log
StreamOrder	Strahler stream order of the focal stream segment.	NHD Plus Version 2 ^b	n/a

ArbolateSum	Total length of all stream segments upstream of the focal stream segment (including the focal segment) in kilometers.	NHD Plus Version 2b	Natural log
AreaCatch	Total surface area of the immediate catchment contributing to a focal stream segment (exclusive of upstream segments), in square kilometers.	StreamCat ^a	Natural log
AreaWater	Total surface area of the watershed contributing to a focal stream segment, in square kilometers.	StreamCat ^a	Natural log
RunoffCatch	Mean annual runoff within the catchment, in millimeters per year.	StreamCat ^a	Natural log
RunoffWater	Mean annual runoff within the watershed, in millimeters per year.	StreamCat ^a	Natural log
Flashiness	Cumulative changes in daily discharge, cumulative discharge for the entire time-series.	Random forest model $(R^2 = 0.709)$	Natural log
HighFlowPulse7	Percent of daily discharge values (within a time-series) that are greater than 7´ the median value.	Random forest model $(R^2 = 0.516)$	Natural log
HighFlowPulse3	Percent of daily discharge values (within a time-series) that are greater than 3´ the median value.	Random forest model $(R^2 = 0.533)$	Natural log
LowFlowPulse	Incidence of daily discharge values that are less than the 25th percentile for the entire time-series.	Random forest model $(R^2 = 0.458)$	Natural log
Minimum30DayFlow	Minimum average discharge that persists for 30 consecutive days within a time-series.	Random forest model $(R^2 = 0.413)$	Natural log
DailyFlowCV	Coefficient of variation in daily discharge.	Random forest model $(R^2 = 0.654)$	Natural log
SedimentAverage	Un-weighted average of sediment size categories, based on the Wentworth scale.	Interpolated from field data	Natural log
SedimentHierarchical	Weighted average of sediment size categories, based on the Wentworth scale.	Interpolated from field data	Natural log
Bioclimate1	Annual mean air temperature, in degrees Celsius.	WorldClim Version 2 (30 second) c	Natural $\log (x + 20)$
Bioclimate2	Mean diurnal range (mean of monthly (max air temp – min air temp)), in degrees Celsius.	WorldClim Version 2 (30 second) c	Natural log
Bioclimate3	Isothermality ((Bioclimate2 , Bioclimate7) ÷ 100)).	WorldClim Version 2 (30 second) c	Natural log
Bioclimate4	Temperature seasonality (standard deviation ÷ 100).	WorldClim Version 2 (30 second) c	Natural log
Bioclimate5	Maximum air temperature of the warmest month, in degrees Celsius.	WorldClim Version 2 (30 second) c	Natural $\log (x + 20)$
Bioclimate6	Minimum air temperature of the coldest month, in degrees Celsius.	WorldClim Version 2 (30 second) c	Natural log $(x + 20)$
Bioclimate7	Annual air temperature range (Bioclimate5 – Bioclimate6), in degrees Celsius.	WorldClim Version 2 (30 second) c	Natural log

Bioclimate8	Mean air temperature of the wettest quarter, indegrees Celsius.	WorldClim Version 2 (30 second) c	Natural log $(x + 20)$
Bioclimate9	Mean air temperature of the driest quarter, in degrees Celsius.	WorldClim Version 2 (30 second) c	Natural $\log (x + 20)$
Bioclimate10	Mean air temperature of the warmest quarter, in degrees Celsius.	WorldClim Version 2 (30 second) c	Natural $\log (x + 20)$
Bioclimate11	Mean air temperature of the coldest quarter, in degrees Celsius.	WorldClim Version 2 (30 second) c	Natural $\log (x + 20)$
Bioclimate12	Annual precipitation, in millimeters per year.	WorldClim Version 2 (30 second) c	Natural log
Bioclimate13	Precipitation of wettest month, in millimeters per month.	WorldClim Version 2 (30 second) c	Natural log
Bioclimate14	Precipitation of driest month, in millimeters per month.	WorldClim Version 2 (30 second) c	Natural log
Bioclimate15	Precipitation seasonality (coefficient of variation among months).	WorldClim Version 2 (30 second) c	Natural log
Bioclimate16	Precipitation of wettest quarter, in millimeters per three months.	WorldClim Version 2 (30 second) c	Natural log
Bioclimate17	Precipitation of driest quarter, in millimeters per three months.	WorldClim Version 2 (30 second) c	Natural log
Bioclimate18	Precipitation of warmest quarter, in millimeters per three months.	WorldClim Version 2 (30 second) ^c	Natural log
Bioclimate19	Precipitation of coldest quarter, in millimeters per three months.	WorldClim Version 2 (30 second) c	Natural log
Precipitation1	Mean January precipitation, in millimeters per year.	WorldClim Version 2 (30 second) c	Natural log
Precipitation2	Mean February precipitation, in millimeters per year.	WorldClim Version 2 (30 second) ^c	Natural log
Precipitation3	Mean March precipitation, in millimeters per year.	WorldClim Version 2 (30 second) c	Natural log
Precipitation4	Mean April precipitation, in millimeters per year.	WorldClim Version 2 (30 second) c	Natural log
Precipitation5	Mean May precipitation, in millimeters per year.	WorldClim Version 2 (30 second) c	Natural log
Precipitation6	Mean June precipitation, in millimeters per year.	WorldClim Version 2 (30 second) c	Natural log
Precipitation7	Mean July precipitation, in millimeters per year.	WorldClim Version 2 (30 second) c	Natural log

Precipitation8	Mean August precipitation, in millimeters per year.	WorldClim Version 2 (30 second) c	Natural log
Precipitation9	Mean September precipitation, in millimeters per year.	WorldClim Version 2 (30 second) c	Natural log
Precipitation10	Mean October precipitation, in millimeters per year.	WorldClim Version 2 (30 second) c	Natural log
Precipitation11	Mean November precipitation, in millimeters per year.	WorldClim Version 2 (30 second) c	Natural log
Precipitation12	Mean December precipitation, in millimeters per year.	WorldClim Version 2 (30 second) c	Natural log
AirTemperature1	Mean January air temperature, in degrees Celsius.	WorldClim Version 2 (30 second) c	Natural $\log (x + 20)$
AirTemperature2	Mean February air temperature, in degrees Celsius.	WorldClim Version 2 (30 second) c	Natural log $(x + 20)$
AirTemperature3	Mean March air temperature, in degrees Celsius.	WorldClim Version 2 (30 second) c	Natural log $(x + 20)$
AirTemperature4	Mean April air temperature, in degrees Celsius.	WorldClim Version 2 (30 second) c	Natural $\log (x + 20)$
AirTemperature5	Mean May air temperature, in degrees Celsius.	WorldClim Version 2 (30 second) c	Natural $\log (x + 20)$
AirTemperature6	Mean June air temperature, in degrees Celsius.	WorldClim Version 2 (30 second) c	Natural $\log (x + 20)$
AirTemperature7	Mean July air temperature, in degrees Celsius.	WorldClim Version 2 (30 second) c	Natural $\log (x + 20)$
AirTemperature8	Mean August air temperature, in degrees Celsius.	WorldClim Version 2 (30 second) c	Natural log $(x + 20)$
AirTemperature9	Mean September air temperature, in degrees Celsius.	WorldClim Version 2 (30 second) c	Natural log $(x + 20)$
AirTemperature10	Mean October air temperature, in degrees Celsius.	WorldClim Version 2 (30 second) c	Natural $\log (x + 20)$
AirTemperature11	Mean November air temperature, in degrees Celsius.	WorldClim Version 2 (30 second) c	Natural $\log (x + 20)$
AirTemperature12	Mean December air temperature, in degrees Celsius.	WorldClim Version 2 (30 second) ^c	Natural $\log (x + 20)$
ImperviousCatch	Mean percent imperviousness of anthropogenic surfaces within the catchment for a focal stream segment. Taken from 2006 Land Cover data.	StreamCat ^a	Arcsine square root
ImperviousWater	Mean percent imperviousness of anthropogenic surfaces within the watershed for a focal stream segment. Taken from 2006 Land Cover data.	StreamCat ^a	Arcsine square root

RoadDensityCatch	Density of roads within the catchment (2010 Census Tiger lines), in kilometers per square kilometer.	StreamCat ^a	Natural log
RoadDensityWater	Density of roads within the watershed (2010 Census Tiger lines), in kilometers per square kilometer.	StreamCat ^a	Natural log
RoadCrossingDensityCatch	Density of road-stream intersections (2010 Census Tiger lines) within the catchment, as number of crossings per square kilometer.	StreamCat ^a	Natural log
RoadCrossingDensityWater	Density of road-stream intersections (2010 Census Tiger lines) within the watershed, as number of crossings per square kilometer.	StreamCat ^a	Natural log
DamDensityCatch	Density of georeferenced dams within the catchment, as number of dams per square kilometer.	StreamCat ^a	Natural log
DamDensityWater	Density of georeferenced dams within the watershed, as number of dams per square kilometer.	StreamCat ^a	Natural log
DamNormalStorageCatch	Total volume all reservoirs (NORM_STORA) within the catchment per unit area of catchment, as cubic meters per square kilometer.	StreamCat ^a	Natural log
DamNormalStorageWater	Total volume all reservoirs (NORM_STORA) within the watershed per unit area of catchment, as cubic meters per square kilometer.	StreamCat ^a	Natural log
PopulationDensityCatch	Mean population density (2010 Census) within the catchment, as number of residents per square kilometer.	StreamCat ^a	Natural log
PopulationDensityWater	Mean population density (2010 Census) within the watershed, as number of residents per square kilometer.	StreamCat ^a	Natural log
HousingDensityCatch	Mean housing unit density within the catchment, as number of housing units per square kilometer.	StreamCat ^a	Natural log
HousingDensityWater	Mean housing unit density within the watershed, as number of housing units per square kilometer.	StreamCat ^a	Natural log
PesticidesCatch	Mean pesticide use within the catchment (1997 records), in kilograms per square kilometer.	StreamCat ^a	Natural log
PesticidesWater	Mean pesticide use within the watershed (1997 records), in kilograms per square kilometer.	StreamCat ^a	Natural log
NPDES_DensityCatch	Density of permitted NPDES (National Pollutant Discharge Elimination System) sites within the catchment, as number of sites per square kilometer.	StreamCat ^a	Natural log
NPDES_DensityWater	Density of permitted NPDES (National Pollutant Discharge Elimination System) sites within the watershed, as number of sites per square kilometer.	StreamCat ^a	Natural log
TRI_DensityCatch	Density of TRI (Toxic Release Inventory) sites within the catchment, as number of sites per square kilometer.	StreamCat ^a	Natural log
TRI_DensityWater	Density of TRI (Toxic Release Inventory) sites within the watershed, as number of sites per square kilometer.	StreamCat ^a	Natural log

SuperfundDensityCatch	Density of Superfund sites within the catchment, as number of sites per square kilometer.	StreamCat ^a	Natural log
SuperfundDensityWater	Density of Superfund sites within the watershed, as number of sites per square kilometer.	StreamCat ^a	Natural log
MinesDensityCatch	Density of permitted mining sites within the catchment, as number of mines per square kilometer.	StreamCat ^a	Natural log
MinesDensityWater	Density of permitted mining sites within the watershed, as number of mines per square kilometer.	StreamCat ^a	Natural log
PctUrbanHighCatch	Percent of catchment classified as developed, high-intensity land use (NLCD 2006 class 24).	StreamCat ^a	Arcsine square root
PctUrbanHighWater	Percent of watershed classified as developed, high-intensity land use (NLCD 2006 class 24).	StreamCat ^a	Arcsine square root
PctUrbanMediumCatch	Percent of catchment classified as developed, medium-intensity land use (NLCD 2006 class 23).	StreamCat ^a	Arcsine square root
PctUrbanMediumWater	Percent of watershed classified as developed, medium-intensity land use (NLCD 2006 class 23).	StreamCat ^a	Arcsine square root
PctUrbanLowCatch	Percent of catchment classified as developed, low-intensity land use (NLCD 2006 class 22).	StreamCat ^a	Arcsine square root
PctUrbanLowWater	Percent of watershed classified as developed, low-intensity land use (NLCD 2006 class 22).	StreamCat ^a	Arcsine square root
PctUrbanOpenCatch	Percent of catchment classified as developed, open space land use (NLCD 2006 class 21).	StreamCat ^a	Arcsine square root
PctUrbanOpenWater	Percent of watershed classified as developed, open space land use (NLCD 2006 class 21).	StreamCat ^a	Arcsine square root
PctCropCatch	Percent of catchment classified as crop land use (NLCD 2006 class 82).	StreamCata	Arcsine square root
PctCropWater	Percent of watershed classified as crop land use (NLCD 2006 class 82).	StreamCata	Arcsine square root
PctHayCatch	Percent of catchment classified as hay land use (NLCD 2006 class 81).	StreamCat ^a	Arcsine square root
PctHayWater	Percent of watershed classified as hay land use (NLCD 2006 class 81).	StreamCat ^a	Arcsine square root
PctDeciduousCatch	Percent of catchment classified as deciduous forest land cover (NLCD 2006 class 41).	StreamCat ^a	Arcsine square root
PctDeciduousWater	Percent of watershed classified as deciduous forest land cover (NLCD 2006 class 41).	StreamCat ^a	Arcsine square root
PctConiferousCatch	Percent of catchment classified as evergreen forest land cover (NLCD 2006 class 42).	StreamCat ^a	Arcsine square root
PctConiferousWater	Percent of watershed classified as evergreen forest land cover (NLCD 2006 class 42).	StreamCat ^a	Arcsine square root
PctMixedForestCatch	Percent of catchment classified as mixed deciduous/evergreen forest land cover (NLCD 2006 class 43).	StreamCat ^a	Arcsine square root

PctMixedForestWater	Percent of watershed classified as mixed deciduous/evergreen forest land cover (NLCD 2006 class 43).	StreamCat ^a	Arcsine square root
PctTotalForestCatch	Sum of PctDeciduousCatch + PctConiferousCatch + PctMixedForestCatch.	Derived from StreamCat ^a	Arcsine square root
PctBarrenLandCatch	Percent of catchment classified as barren land cover (NLCD 2006 class 31).	StreamCat ^a	Arcsine square root
PctBarrenLandWater	Percent of watershed classified as barren land cover (NLCD 2006 class 31).	StreamCat ^a	Arcsine square root
PctOpenWaterCatch	Percent of catchment classified as open water land cover (NLCD 2006 class 11).	StreamCat ^a	Arcsine square root
PctOpenWaterWater	Percent of watershed classified as open water land cover (NLCD 2006 class 11).	StreamCat ^a	Arcsine square root
PctIceCatch	Percent of catchment classified as ice/snow land cover (NLCD 2006 class 12).	StreamCat ^a	Arcsine square root
PctIceWater	Percent of watershed classified as ice/snow land cover (NLCD 2006 class 12).	StreamCat ^a	Arcsine square root
PctHerbWetlandCatch	Percent of catchment classified as herbaceous wetland land cover (NLCD 2006 class 95).	StreamCat ^a	Arcsine square root
PctHerbWetlandWater	Percent of watershed classified as herbaceous wetland land cover (NLCD 2006 class 95).	StreamCat ^a	Arcsine square root
PctWoodWetlandCatch	Percent of catchment classified as woody wetland land cover (NLCD 2006 class 90).	StreamCat ^a	Arcsine square root
PctWoodWetlandWater	Percent of watershed classified as woody wetland land cover (NLCD 2006 class 90).	StreamCat ^a	Arcsine square root
PctShrubCatch	Percent of catchment classified as shrub/scrub land cover (NLCD 2006 class 52).	StreamCat ^a	Arcsine square root
PctShrubWater	Percent of watershed classified as shrub/scrub land cover (NLCD 2006 class 52).	StreamCat ^a	Arcsine square root
PctGrasslandCatch	Percent of catchment classified as grassland/herbaceous land cover (NLCD 2006 class 71).	StreamCat ^a	Arcsine square root
PctGrasslandWater	Percent of watershed classified as grassland/herbaceous land cover (NLCD 2006 class 71).	StreamCat ^a	Arcsine square root
PctCarbonateResidualCatch	Percent of catchment classified as lithology type: carbonate residual material.	StreamCat ^a	Arcsine square root
PctCarbonateResidualWater	Percent of watershed classified as as lithology type: carbonate residual material.	StreamCat ^a	Arcsine square root
PctNonCarbonateResidualCatch	Percent of catchment classified as lithology type: non-carbonate residual material.	StreamCat ^a	Arcsine square root

PctNonCarbonateResidualWater	Percent of watershed classified as as lithology type: non-carbonate residual material.	StreamCat ^a	Arcsine square root
PctAlkalineIntrusiveVolcanicCatch	Percent of catchment classified as lithology type: alkaline intrusive volcanic rock.	StreamCat ^a	Arcsine square root
PctAlkalineIntrusiveVolcanicWater	volcanic rock.	StreamCat ^a	Arcsine square root
PctSilicicCatch	Percent of catchment classified as lithology type: silicic residual material.	StreamCat ^a	Arcsine square root
PctSilicicWater	Percent of watershed classified as as lithology type: silicic residual material.	StreamCat ^a	Arcsine square root
PctExtrusiveVolcanicCatch	Percent of catchment classified as lithology type: extrusive volcanic rock.	StreamCat ^a	Arcsine square root
PctExtrusiveVolcanicWater	Percent of watershed classified as as lithology type: extrusive volcanic rock.	StreamCat ^a	Arcsine square root
PctColluvialSedimentCatch	Percent of catchment classified as lithology type: colluvial sediment.	StreamCat ^a	Arcsine square root
PctColluvialSedimentWater	Percent of watershed classified as as lithology type: colluvial sediment.	StreamCat ^a	Arcsine square root
PctGlacialTillClayCatch	Percent of catchment classified as lithology type: glacial till, clayey.	StreamCat ^a	Arcsine square root
PctGlacialTillClayWater	Percent of watershed classified as as lithology type: glacial till, clayey.	StreamCat ^a	Arcsine square root
PctGlacialTillLoamyCatch	Percent of catchment classified as lithology type: glacial till, loamy.	StreamCat ^a	Arcsine square root
PctGlacialTillLoamyWater	Percent of watershed classified as as lithology type: glacial till, loamy.	StreamCat ^a	Arcsine square root
PctGlacialTillCoarseCatch	Percent of catchment classified as lithology type: glacial till, coarse-textured.	StreamCat ^a	Arcsine square root
PctGlacialTillCoarseWater	Percent of watershed classified as as lithology type: glacial till, coarse-textured.	StreamCat ^a	Arcsine square root
PctGlacialLakeCoarseCatch	Percent of catchment classified as lithology type: glacial outwash and glacial lake sediment, coarse-textured.	StreamCat ^a	Arcsine square root
PctGlacialLakeCoarseWater	Percent of watershed classified as as lithology type: glacial outwash and glacial lake sediment, coarse-textured.	StreamCat ^a	Arcsine square root
PctGlacialLakeFineCatch	Percent of catchment classified as lithology type: glacial lake sediment, fine-textured.	StreamCat ^a	Arcsine square root
PctGlacialLakeFineWater	Percent of watershed classified as as lithology type: glacial lake sediment, fine-textured.	StreamCat ^a	Arcsine square root
PctHydricCatch	Percent of catchment classified as lithology type: hydric, peat and muck.	StreamCat ^a	Arcsine square root
PctHydricWater	Percent of watershed classified as as lithology type: hydric, peat and muck.	StreamCat ^a	Arcsine square root
PctEolianCoarseCatch	Percent of catchment classified as lithology type: eolian sediment, coarse-textured (sand dunes).	StreamCat ^a	Arcsine square root
PctEolianCoarseWater	Percent of watershed classified as as lithology type: eolian sediment, coarse-textured (sand dunes).	StreamCat ^a	Arcsine square root
PctEolianFineCatch	Percent of catchment classified as lithology type: eolian sediment, fine-textured (glacial loess).	StreamCat ^a	Arcsine square root

PctEolianFineWater	Percent of watershed classified as as lithology type: eolian sediment, fine-textured (glacial loess).	StreamCat ^a	Arcsine square root
PctSalineLakeCatch	Percent of catchment classified as lithology type: saline lake sediment.	StreamCata	Arcsine square root
PctSalineLakeWater	Percent of watershed classified as as lithology type: saline lake sediment.	StreamCat ^a	Arcsine square root
PctAlluviumCoastalCatch	Percent of catchment classified as lithology type: alluvium and fine-textured coastal zone sediment.	StreamCat ^a	Arcsine square root
PctAlluviumCoastalWater	Percent of watershed classified as as lithology type: alluvium and fine- textured coastal zone sediment.	StreamCat ^a	Arcsine square root
PctCoastalCoarseCatch	Percent of catchment classified as lithology type: coastal zone sediment, coarse-textured.	StreamCat ^a	Arcsine square root
PctCoastalCoarseWater	Percent of watershed classified as as lithology type: coastal zone sediment, coarse-textured.	StreamCat ^a	Arcsine square root
PctWaterCatch	Percent of catchment classified as lithology type: water.	StreamCata	Arcsine square root
PctWaterWater	Percent of watershed classified as as lithology type: water.	StreamCat ^a	Arcsine square root
WaterTableDepthCatch	Mean seasonal water table depth of soils (STATSGO) within catchment, in centimeters.	StreamCat ^a	Natural log
WaterTableDepthWater	Mean seasonal water table depth (cm) of soils (STATSGO) within watershed, in centimeters.	StreamCat ^a	Natural log
OrganicMatterCatch	Mean organic matter content of soils (STATSGO) within catchment, as percent by weight.	StreamCat ^a	Natural log
OrganicMatterWater	Mean organic matter content of soils (STATSGO) within watershed, as percent by weight.	StreamCat ^a	Natural log
PermeabilityCatch	Mean permeability of soils (STATSGO) within catchment, in centimeters per hour.	StreamCat ^a	Natural log
PermeabilityWater	Mean permeability of soils (STATSGO) within watershed, in centimeters per hour.	StreamCat ^a	Natural log
BedrockDepthCatch	Mean depth to bedrock (STATSGO) within catchment, in centimeters.	StreamCat ^a	Natural log
BedrockDepthWater	Mean depth to bedrock (STATSGO) within watershed, in centimeters.	StreamCat ^a	Natural log
ClayCatch	Mean percent clay content of soils (STATSGO) within catchment.	StreamCata	Natural log
ClayWater	Mean percent clay content of soils (STATSGO) within watershed.	StreamCata	Natural log
SandCatch	Mean percent sand content of soils (STATSGO) within catchment.	StreamCat ^a	Natural log
SandWater	Mean percent sand content of soils (STATSGO) within watershed.	StreamCat ^a	Natural log

a – http://newftp.epa.gov/EPADataCommons/ORD/NHDPlusLandscapeAttributes/StreamCat/WelcomePage.html
 b – http://www.horizon-systems.com/NHDPlus/
 c – http://worldclim.org/version2